SEMARAK ILMU PUBLISHING

Journal of Advanced Research in Applied Mechanics

Journal homepage:
https://semarakilmu.com.my/journals/index.php/appl_mech/index
ISSN: 2289-7895

Spectral Analysis of Fiber Bragg Grating Sensor on Glass Fiber Reinforced Polymer

Miminorazeansuhaila Loman[1], Mohamad Hafizi Zohari[1,*], Fauziana Lamin[2]

[1] Faculty of Mechanical Engineering & Automotive Technology, Universiti Malaysia Pahang Al-Sultan Abdullah, 26600 Pekan, Pahang, Malaysia
[2] Vehicle Safety and Biomechanics Research Centre, Malaysian Institute of Road Safety Research, Lot 125-135, Jalan TKS 1, Taman Kajang Sentral, 43000 Kajang, Selangor, Malaysia

ARTICLE INFO

Article history:
Received 26 October 2024
Received in revised form 27 November 2024
Accepted 4 December 2024
Available online 30 December 2024

Keywords:
Fatigue; Fiber Bragg Grating sensor; strain; spectral analysis; wavelength shift; structural health monitoring

ABSTRACT

An effective technique must be utilized to monitor composites' health as its application in engineering constructions grows to avoid sudden failure as it degrades. In line with that, this study analyses the progress of fatigue strain on GFRP specimens during fatigue tests using the FBG wavelength shifts parameter. Its purpose was to monitor the FBG wavelength shifts during three stages of fatigue test. Fatigue test specimens were firstly fabricated using the hand layup technique. Tensile and fatigue tests were conducted on the fabricated GFRP specimens. The FBG wavelength spectrums were acquired using the FBG sensor during the fatigue test of each specimen at 40% stress amplitudes. Spectral analysis was then carried out to characterize the FBG spectrum as the fatigue failure progresses. As a result, the FBG wavelength shifted each time the stress amplitudes were applied to the GFRP fatigue test specimen. The GFRP specimen that was applied with 40% of the ultimate stress was presented. These shifts and changes were observed at the early, middle, and final stages of the fatigue test. Wavelength shifts were not obvious in the early stage but abrupt in the middle and final stage of fatigue test of the GFRP specimen.

1. Introduction

A composite material that mixes polyester with E-glass material is called glass fiber reinforced polymer (GFRP), also known as glass fiber reinforced plastic. GFRP has been prepared by various manufacturing technology and is commonly used in various applications. Glass fiber has excellent qualities such as strong strength, flexibility, stiffness, and chemical resistance [1]. There are many varieties of glass fiber, and each has unique characteristics such being lightweight, low in density, and highly durable. For applications needing high strength-to-weight ratios and extra mechanical properties, it may also be used as a substitute for conventional reinforcement materials in composites. If the composite is stronger than the unreinforced matrix, the interfacial bond strength must be high enough for the load to be transferred from the matrix to the fibers [2,3]. While

* *Corresponding author.*
E-mail address: hafizi@umpsa.edu.my

https://doi.org/10.37934/aram.130.1.7279

considering the composites' toughness, the interface shouldn't be too robust to prevent toughening mechanisms like debonding from occurring. The most significant factor determining the composite properties is typically thought to be the volume fraction. Additionally, homogeneity is a crucial factor in determining how much the physical and mechanical properties of a representative volume of the material may vary from those of the material's average.

One of the major challenges in the marine energy industry is the ability to predict fatigue failure of its composite structures [4]. Tidal turbine blades are usually made of glass fiber-reinforced epoxy resin composites, and the main fatigue failure types include delamination and fiber breaking [5]. To deal with these challenges, reliable and responsive structural health monitoring (SHM) is vital. A very intriguing instrument for applications involving structural health monitoring involving SHM is fiber Bragg grating (FBG) sensors. FBG sensors are primarily used in SHM systems for strain [6] and temperature [7] measurements. FBG sensors' primary advantages include its small size, high multiplexing capacity, corrosion resistance, and lack of calibration needs [8]. FBG sensors may be affixed to component or structure surfaces [9–11] or implanted during the production of the material [12,13]. In real engineering applications, FBGs are typically utilised as quasi-distributed sensors to detect structural damage caused by central wavelength shifts. It is discovered that the non-uniform strain field created by the crack can also affect the FBG reflection spectra [14]. According to Mieloszyk's [15] analysis, there was good agreement between the fatigue force profile and the strain curves measured by the FBG sensors for a sample of aluminium alloy used in the Mi-2 helicopter rotor blade. This prior study demonstrates the possibility of FBG signal for fatigue monitoring even if the strain curves were almost insensitive to the fracture propagation process until the final stage of the test, when the crack length was 25 mm long.

In this study, spectral analysis of FBG signals was conducted. By considering the existence of wavelength shift [16] and the power reflected varies as fatigue failure progress, the integration of area under the curve of FBG wavelength spectrum parameter on the SHM was explored. For that reason, fatigue loading conditions of 40% of the ultimate stress were considered to replicate a fatigue failure progress. This loading condition was considered for the spectral analysis as it has an adequate time to failure as compared to the higher stress amplitude and therefore distinctive fatigue stages are present. Whereas for the lower loading condition that recorded a longer time to failure, the number of data counts is considerably higher. Therefore, the selected loading is assumed to be optimal for the exploration of the FBG spectral analysis.

2. Materials and Methods

2.1 FBG Principles

The FBG sensor is a permanent, periodical perturbation in the index of refraction of the optical fiber core. A narrow bandwidth of wavelengths are reflected while all other wavelengths are transmitted when a wide spectrum of wavelengths is passed through the FBG [18]. In other words, the reflected power is equal to the input power minus the transmitted power. The wavelength at maximum reflectivity is referred to as the Bragg wavelength, λ_B and is determined by the condition:

$$\lambda_B = 2n_{eff}\Lambda \tag{1}$$

where Λ is the period of the index of refraction variation and n_{eff} is the effective refractive index. Eq. (1), also known as the Bragg reflection wavelength, is the peak wavelength of the narrowband spectral component reflected by the FBG [19]. As an axial strain, ε is applied to the FBG, the Bragg

wavelength shifts to lower wavelengths (compression) or higher wavelengths (tension). The wavelength of FBG changes with strain and temperature according to Eq. (2)

$$\frac{\Delta\lambda}{\lambda_0} = k\varepsilon + \alpha_\delta \Delta T \tag{2}$$

where $\Delta\lambda$ is the wavelength shift, λ_0 is the wavelength at starting of a test, *k = 1- p* where p is the photo elastic coefficient (p=0.22) and k is the gage factor (*k* = 0.78), ε is strain, ΔT is temperature changes in *k* and $\alpha_\delta$is the change in refraction index.

According to coupled-mode theory [20], the grating period and effective refractive index are two physical characteristics of fiber that affect Bragg wavelength. When there is a parameter such as temperature, strain, humidity, pressure, and others are being monitored, the changes of the FBG effective refractive index or the period of the gratings will cause the wavelength of the reflected spectrum shifts to the left or right of the central wavelength. This study emphasizes the applicability of the FBG sensor to detect and characterize the fatigue failure on the GFRP specimen using its wavelength spectrum shifts and its intensity value changes.

2.2 Experimental Setup

This study utilizes the uniform single-mode FBG sensor to detect the strain on the GFRP specimen during the fatigue test. The uniform FBG sensor is characterized by periodic perturbation of the refractive index and works on the principle of Bragg's law [17]. The dimension of the fatigue test specimen is shown in Figure 1. Prior to the fatigue test, the specimen with similar dimensions was statically tested using a tensile test to determine the ultimate strength of the fabricated GFRP. During the fatigue test, the specimen was applied with stress at 40% of the ultimate strength of the fabricated GFRP. The load was applied using a 100 kN capacity of an Instron universal testing machine. The amplitude of the controller could be adjusted to achieve the desired stress. The resultant strain induced in the FBG sensor was measured continuously using the FBG interrogation system. In order to gain the FBG spectrum on the GFRP specimen, the sensor was bonded to the gauge section of the GFRP specimen during the fatigue test. The unstrained center Bragg wavelength for all the FBGs tested during the fatigue test was between 1547 and 1550 nm, meaning the anticipated strain was well within the range of the interrogator.

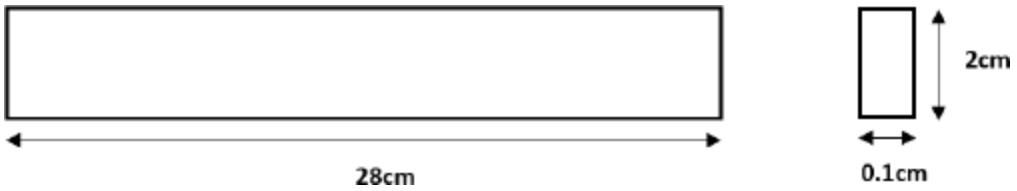

Fig. 1. Dimension of GFRP specimen

3. Results

3.1 Composite Fatigue Failure

Figure 2 shows the GFRP specimen that failed due to fatigue load. It can be seen in the figure that the glass fiber breaks and spreads in between the matrix that holding it.

Fig. 2. Failed GFRP specimen

3.2 FBG Wavelength Shifts

Table 1 summarises the largest peak wavelength for every 30 data counts, λ_{max}, wavelength shift, $\Delta\lambda$ and the respective average area under curve for every 30 data counts, *A.* It exhibits the earliest data obtained as soon as the fatigue test at 40% stress amplitude was commenced. The area under curve, *A* of the wavelength spectrum varied throughout the process. This is because the amount of energy transmitted directly affected the amount of energy reflected in the wavelength during the fatigue test process. Figure 3 shows the FBG wavelength shift during the early stage of the fatigue test on the GFRP specimen that had 40% of the maximum stress applied to it. A total of 150 data counts at the early stage of the fatigue were compared to the first peak wavelength as soon as the test was started. The first peak wavelength at the first data count was 1547.325 nm and labelled as 1 in Figure 3. After some duration which was in the data count range of 15 to 45, the largest wavelength shift was 2.261 nm at 1549.586 nm. The wavelength shift was then increased to 3.162 nm in the range of data count 46 to 76 at the peak wavelength of 1550.487 nm. The wavelength shift increased to 5.393 nm in the following range of 77 to 107 data counts. In the last range of the early stage of fatigue test which was between 139 to 169 data counts, the wavelength shifts were the largest which were 5.839 and 6.282 nm, respectively. At this early stage of fatigue test, the GFRP might undergo elastic deformation and the wavelength shifts were fluctuating between 2 to 6 nm. The entire spectrum of recorded wavelength shifts was moved positively to the right region of the FBG wavelength spectrum. The area, *A* in Table 1 represents the area under the FBG wavelength spectrum curve. The A values varied throughout early stage of the fatigue test from 1.64E06 until 1.655E06.

Table 1
FBG wavelength shifts during the early stage of the fatigue test for 40% stress amplitude

Data count range	λ_{max}	$\Delta\lambda$ (nm)	Area, A
15-45	1549.586	2.261	1.647E06
46-76	1550.487	3.162	1.642E06
77-107	1552.718	5.393	1.641E06
108-138	1553.164	5.839	1.640E06
139-169	1553.607	6.282	1.655E06

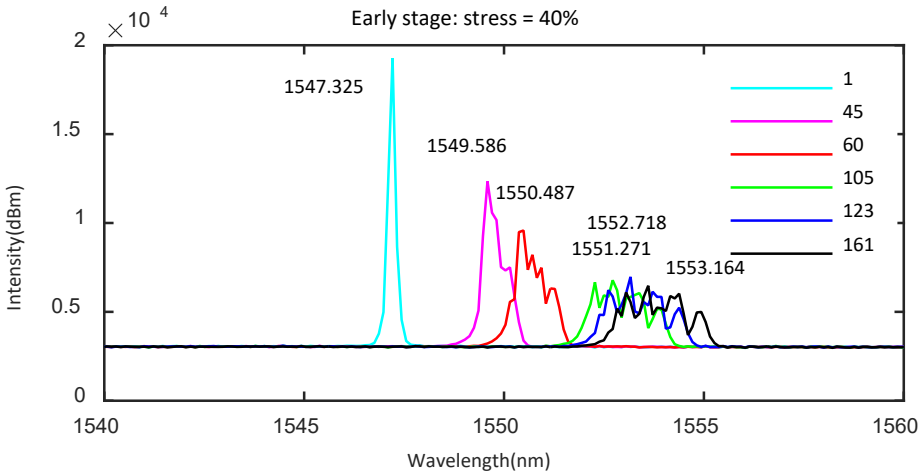

Fig. 3. FBG wavelength shift for 150 data counts at early stage of fatigue test for specimen at 40% stress amplitude

Next, the FBG signal recorded during the middle stage of the fatigue test was monitored and presented in Table 2. The distribution of area under curve for the FBG wavelength was also variedly tabulated in Table 2. In Figure 4, the wavelength was recorded shifted for 6.905 nm from 1547.325 nm in the range of 31865 to 31894. The largest shift in the 30 data count range was at 31894 data count. A similar shift direction happened to the data count range of 31895 to 31924 and 31955 to 31984 in Figure 4 for wavelength shift of 6.794 nm. It can be observed that the peak wavelength was then shifted for 6.906 nm in the data count range of 31955 to 31985. Lastly, in the range of 31985 to 32000 data counts, the wavelength was static and did not change from its previous position which was 6.906 nm at 31996 data count. At this stage, the FBG wavelength shifts seemed to be abrupt and the shifts were mostly above 6 nm as tabulated in Table 2. In the middle stage of the fatigue test, the GFRP specimen may already experience the fatigue crack initiation and propagation which explained the bigger range of wavelength shift compared to the early stage of the fatigue test. The fatigue cracks might start to propagate and the FBG shifts farther form its original position every time the fatigue load was applied. This was proved by the wavelength shifts that ranges above 6.5 nm. These shifts were larger than the wavelength shifts in the early stage of fatigue test which was varied in the range of 2 to 6.3 nm. The area under curve, A seems varied throughout the fatigue test in the range of 2.082E06 to 2.194E06 which is higher than in the early stage of fatigue test.

Table 2
FBG wavelength shifts during the middle stage of the fatigue test at 40% stress amplitude

Data count range	λ	$\Delta\lambda$ (nm)	Area, A
31865-31894	1554.23	6.905	2.151E06
31895-31924	1554.119	6.794	2.194E06
31925-31954	1554.119	6.794	2.127E06
31955-31984	1554.23	6.905	2.082E06
31985-32000	1554.23	6.905	2.097E06

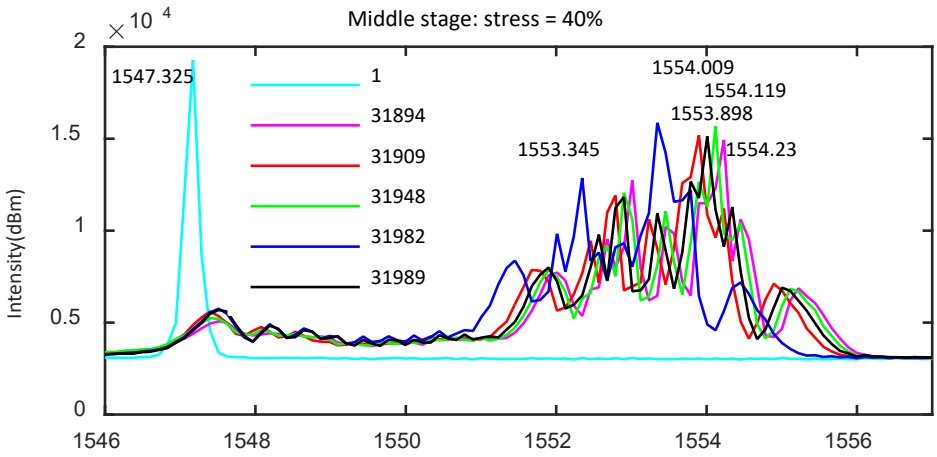

Fig. 4. FBG wavelength shift for 150 data counts at middle stage of fatigue test for 40% stress amplitude

In the final stage of the fatigue test on the GFRP specimen that was applied with 40% stress amplitude, the wavelength was recorded shifted from the original position at 1547.325 nm to the right and left positions. It can be seen in Table 3 that in the data count range of 68399 to 68428, the wavelength shifts to the left position to 1544.312 nm for 3.013 nm (Figure 5). The negative symbol represents the direction of the FBG wavelength shift. This is considered as the farthest shift from its original position for thirty data counts. In the data counts if 30, the peak wavelength was then shifts to the right position and the largest shift was 2.896 nm at 1550.221 nm. The peak wavelength was then shift further for 4.126 nm at 1551.451 nm to the right. It was the shifted to the left position for 2.209 nm at 1545.116 nm. In the last section of data counts, the peak wavelength shifts to the right at 1549.884 nm for 2.559 nm. at this stage, the GFRP specimen might already failed at any moments. As shown in Table 3, the range of the FBG wavelength shifts was varied between 2.209 to 4.126 nm but in both directions unlike in the previous two stages. For the area under curve, A, the values were in the range of 2.125E06 to 2.197E06 and averagely higher than in the early and middle stages.

Table 3
FBG wavelength shifts during the final stage of the fatigue test at 40% stress amplitude

Data count range	λ	$\Delta\lambda$ (nm)	Area, A
68399-68428	1544.312	-3.013	2.181E06
68429-68458	1550.221	2.896	2.125E06
68459-68488	1551.451	4.126	2.149E06
68489-68518	1545.116	-2.209	2.197E06
68519-68548	1549.884	2.559	2.166E06

These wavelength shifts and differences also can be used to classify the fatigue crack initiation on the GFRP specimen. Further observations could be made to determine the detailed distribution of the area under curve value of the FBG wavelength spectrum. This finding demonstrates the feasibility of the FBG wavelength shift for fatigue failure monitoring. The indirect and non-destructive sensing method is valuable for SHM application, especially in monitoring brittle structures like GFRP material.

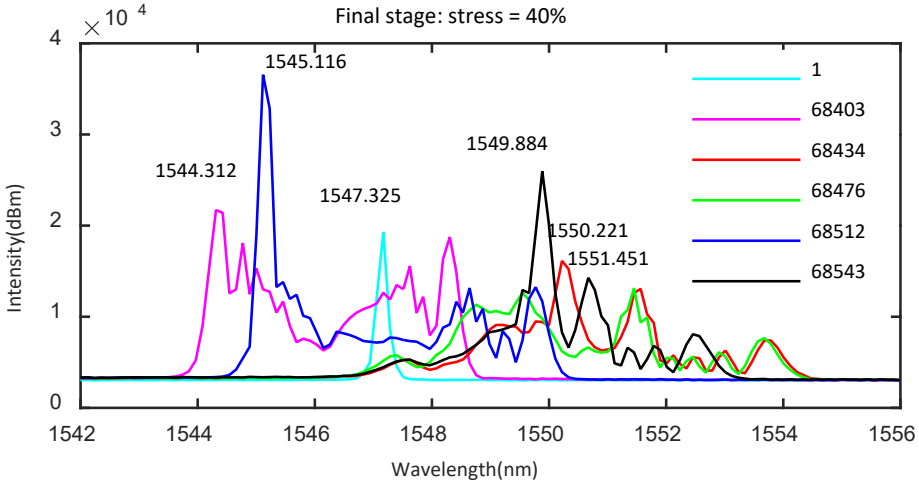

Fig. 5. FBG wavelength shift for 150 data counts at final stage of fatigue test at 40% stress amplitude

4. Conclusions

An experimental study on Fiber Bragg Grating was carried out which provides information on the FBG response spectrum as a result of the applied fatigue load on the GFRP structure. The peak FBG wavelength shifts were observed over time during the progress of the fatigue test on all the GFRP specimens and the result of the specimen that was applied with 40% of ultimate load was presented. The tabulation of FBG wavelength shifts were moderate at the early stage, increasing in the middle stage and slowly decreasing in the final stage of the fatigue test. These shifts can clearly show the progress of fatigue failure on the GFRP specimen as presented in the results section. For area under the curve, A, the values were low in the middle stage and variedly increasing in the middle and final stage of the fatigue test. The parameter that directly connected to the GFRP show that FBG is applicable in detecting the changes in the physical activity of the composite structures. The challenge of this study is that the number of data were quite large and more times were needed for the spectrum processing. On top of that, more studies are needed to develop sensors that is reliable even under high number of cycles for a long duration in SHM.

Acknowledgement

This research received financial support from the Ministry of Higher Education Malaysia under the Fundamental Research Grant Scheme FRGS/1/2019/TK03/UMP/02/7 @ RDU1901116. The authors also would like to thank University of Malaysia Pahang Sultan Abdullah for funding RDU190353.

References

[1] Morampudi, Priyadarsini, Kiran Kumar Namala, Yeshwanth Kumar Gajjela, Majjiga Barath, and Ganaparthy Prudhvi. "Review on glass fiber reinforced polymer composites." *Materials Today: Proceedings* 43 (2021): 314-319. https://doi.org/10.1016/j.matpr.2020.11.669

[2] Chamis, Christos C. *Mechanics of load transfer at the fiber/matrix interface*. National Aeronautics and Space Administration, 1972.

[3] Lee, Ching Hao, Abdan Khalina, and Seng Hua Lee. "Importance of interfacial adhesion condition on characterization of plant-fiber-reinforced polymer composites: A review." *Polymers* 13, no. 3 (2021): 438. https://doi.org/10.3390/polym13030438

[4] Gonabadi, Hassan, Adrian Oila, Arti Yadav, and Steve Bull. "Fatigue damage analysis of GFRP composites using digital image correlation." *Journal of Ocean Engineering and Marine Energy* 7, no. 1 (2021): 25-40. https://doi.org/10.1007/s40722-020-00184-6

[5] Boisseau, Amélie, Peter Davies, and Frédéric Thiebaud. "Fatigue behaviour of glass fibre reinforced composites for ocean energy conversion systems." *Applied Composite Materials* 20 (2013): 145-155. https://doi.org/10.1007/s10443-012-9260-0
[6] Wu, Bitao, Gang Wu, and Caiqian Yang. "Parametric study of a rapid bridge assessment method using distributed macro-strain influence envelope line." *Mechanical Systems and Signal Processing* 120 (2019): 642-663. https://doi.org/10.1016/j.ymssp.2018.10.039
[7] Chen, Junlei, Jihui Wang, Xiaoyang Li, Liangliang Sun, Shuxin Li, and Anxin Ding. "Monitoring of temperature and cure-induced strain gradient in laminated composite plate with FBG sensors." *Composite Structures* 242 (2020): 112168. https://doi.org/10.1016/j.compstruct.2020.112168
[8] Udd, Eric, and William B. Spillman Jr, eds. *Fiber optic sensors: an introduction for engineers and scientists*. John Wiley & Sons, 2024. https://doi.org/10.1002/9781119678892
[9] Fernández, Rosario, Nicolás Gutiérrez, Humberto Jiménez, Fernando Martín, Luis Rubio, José D. Jiménez-Vicaria, Carlo Paulotto, and Fernando Lasagni. "On the structural testing monitoring of CFRP cockpit and concrete/CFRP pillar by FBG sensors." *Advanced engineering materials* 18, no. 7 (2016): 1289-1298. https://doi.org/10.1002/adem.201600065
[10] Mieloszyk, Magdalena, and Wiesław Ostachowicz. "An application of Structural Health Monitoring system based on FBG sensors to offshore wind turbine support structure model." *Marine Structures* 51 (2017): 65-86. https://doi.org/10.1016/j.marstruc.2016.10.006
[11] Chan, Tommy HT, Ling Yu, Hwa-Yaw Tam, Yi-Qing Ni, S. Y. Liu, W. H. Chung, and L. K. Cheng. "Fiber Bragg grating sensors for structural health monitoring of Tsing Ma bridge: Background and experimental observation." *Engineering structures* 28, no. 5 (2006): 648-659. https://doi.org/10.1016/j.engstruct.2005.09.018
[12] Mieloszyk, Magdalena, Katarzyna Majewska, and Wieslaw Ostachowicz. "Application of embedded fibre Bragg grating sensors for structural health monitoring of complex composite structures for marine applications." *Marine structures* 76 (2021): 102903. https://doi.org/10.1016/j.marstruc.2020.102903
[13] Gebremichael, Y. M., W. Li, W. J. O. Boyle, B. T. Meggitt, K. T. V. Grattan, B. McKinley, G. F. Fernando et al. "Integration and assessment of fibre Bragg grating sensors in an all-fibre reinforced polymer composite road bridge." *Sensors and Actuators A: Physical* 118, no. 1 (2005): 78-85. https://doi.org/10.1016/S0924-4247(04)00546-1
[14] Jin, Xin, Shenfang Yuan, and Jian Chen. "On crack propagation monitoring by using reflection spectra of AFBG and UFBG sensors." *Sensors and Actuators A: Physical* 285 (2019): 491-500. https://doi.org/10.1016/j.sna.2018.11.052
[15] Mieloszyk, Magdalena. "Fatigue crack propagation monitoring using fibre Bragg grating sensors." *Vibration* 4, no. 3 (2021): 700-721. https://doi.org/10.3390/vibration4030039
[16] Loman, Miminorazeansuhaila, and Mohd Hafizi Zohari. "Fatigue Detection on Glass Fibre Reinforced Polymer Material Using Fiber Bragg Grating Sensor." In *Symposium on Damage Mechanism in Materials and Structures*, pp. 115-125. Cham: Springer International Publishing, 2020. https://doi.org/10.1007/978-3-030-85646-5_9
[17] Sahota, Jasjot K., Neena Gupta, and Divya Dhawan. "Fiber Bragg grating sensors for monitoring of physical parameters: A comprehensive review." *Optical Engineering* 59, no. 6 (2020): 060901-060901. https://doi.org/10.1117/1.OE.59.6.060901
[18] Peters, Kara, and Daniele Inaudi. "Optical fiber sensors." In *Sensor technologies for civil infrastructures*, pp. 113-147. Woodhead Publishing, 2022. https://doi.org/10.1016/B978-0-08-102696-0.00005-1
[19] Werneck, Marcelo M., R. C. S. B. Allil, Bessie A. Ribeiro, and Fábio VB de Nazaré. "A guide to fiber Bragg grating sensors." *Current trends in short-and long-period fiber gratings* (2013): 1-24.
[20] McCall, Martin. "On the application of coupled mode theory for modeling fiber Bragg gratings." *Journal of Lightwave Technology* 18, no. 2 (2000): 236. https://doi.org/10.1109/50.822798